

N 62 70179

NASA MEMO 2-7-59L

NASA MEMO 2-7-59L

10-27  
344-487

# NASA

## MEMORANDUM

LOW-SPEED YAWED-ROLLING CHARACTERISTICS OF A PAIR OF  
56-INCH-DIAMETER, 32-PLY-RATING, TYPE VII AIRCRAFT TIRES

By Wilbur E. Thompson and Walter B. Horne

Langley Research Center  
Langley Field, Va.

NATIONAL AERONAUTICS AND  
SPACE ADMINISTRATION

WASHINGTON  
February 1959



NATIONAL AERONAUTICS AND SPACE ADMINISTRATION

---

MEMORANDUM 2-7-59L

---

LOW-SPEED YAWED-ROLLING CHARACTERISTICS OF A PAIR OF  
56-INCH-DIAMETER, 32-PLY-RATING, TYPE VII AIRCRAFT TIRES

By Wilbur E. Thompson and Walter B. Horne

SUMMARY

The low-speed (up to 4 miles per hour) yawed-rolling characteristics of two 56 x 16 32-ply-rating, type VII aircraft tires under straight-yawed rolling were determined over a range of inflation pressures and yaw angles for a vertical load approximately equal to 75 percent of the rated vertical load. The quantities measured or determined included cornering force, drag force, self-alining torque, pneumatic caster, vertical tire deflection, yaw angle, and relaxation length.

During straight-yawed rolling the normal force generally increased with increasing yaw angle within the test range. The self-alining torque increased to a maximum value and then decreased with increasing angle of yaw. The pneumatic caster tended to decrease with increasing yaw angle.

INTRODUCTION

In order to cope with airplane landing and taxiing problems such as landings with yaw, wheel shimmy, and ground handling, designers of landing gear must have reliable data on the elastic properties of aircraft tires under such conditions. Until recently, the experimental data on such tire elastic properties, most of which are summarized and discussed in reference 1, were limited in both scope and quantity. A program was initiated by the Langley Research Center to alleviate this lack of experimental data by determining experimental values of some of the essential tire parameters.

Most of the static-force-deflection tests of this program have been completed and the results are reported in reference 2. Low-speed yawed-rolling and some other elastic characteristics were reported in references 3, 4, and 5, respectively, for pairs of 56-inch-diameter, 24-ply-rating, 26-inch, 12-ply-rating, and 40-inch, 14-ply-rating type VII tires. These and available data from other American and foreign sources

are summarized in reference 6 which also gives empirical methods for determining these tire characteristics. The present paper gives results from the kinematic test program for a pair of 56-inch-diameter, 32-ply-rating type VII aircraft tires, and completes the kinematic part of the program. (The static characteristics of this size tire are reported in reference 2.)

The investigation consisted of towing the tire specimens along a straight path in a yawed condition. The angle-of-yaw range covered was from  $1.75^\circ$  to  $10.5^\circ$  and the inflation-pressure range was from about 160 pounds per square inch to 240 pounds per square inch. The vertical loading condition investigated was 45,000 pounds per tire; this value represented 75 percent of the rated load for this type of tire as specified by reference 7. Power and strength limitations of test equipment prevented testing at yaw angles greater than  $10.5^\circ$  and vertical loads greater than 45,000 pounds per wheel. For each yawed-rolling run, the towing speed was held constant and did not exceed 4 miles per hour. The quantities measured or determined included vertical tire deflection, cornering force, drag force, self-aligning torque, pneumatic caster, and relaxation length.

#### SYMBOLS

$d$	outside diameter of free tire, $\frac{\text{Tire circumference}}{\pi}$ , in.
$F_R$	resultant force, $\sqrt{F_x^2 + F_y^2}$ , lb
$F_x$	instantaneous drag or fore-and-aft force (ground force parallel to direction of motion), lb
$F_y$	instantaneous cornering force (ground force perpendicular to direction of motion), lb
$F_z$	vertical load on tire, lb
$F_\psi$	normal force (ground force perpendicular to wheel plane, $F_y \cos \psi + F_x \sin \psi$ ), lb
$2h$	overall tire-ground contact length, in.
$L_y$	yawed-rolling relaxation length, in.

$M_z$	self-aligning torque, lb-in.
$N$	cornering power (rate of change of cornering force with yaw angle for small yaw angles on a rolling tire, $dF_y,r,e/d\psi$ or $dF_{\psi,r,e}/d\psi$ for $\psi$ approaching 0), lb/deg
$p$	tire inflation pressure, lb/sq in.
$p_r$	rated tire inflation pressure, lb/sq in.
$p_0$	tire inflation pressure at zero vertical load ( $F_z = 0$ ), lb/sq in.
$q$	pneumatic caster, $M_{z,r,e}/F_{\psi,r,e}$ , in.
$r$	radius of free tire, in.
$w$	maximum tire width, in.
$x$	displacement in direction of motion, in. or ft
$\delta$	vertical tire deflection due to combined vertical and yaw loads, in.
$\delta_b$	vertical deflection at tire bottoming, in.
$\delta_0$	vertical tire deflection due to vertical load only, in.
$\mu_{\psi}$	yawed-rolling coefficient of friction
$\psi$	yaw angle, deg

Subscripts:

$e$	equilibrium or steady-state rolling condition
$m$	maximum
$r$	rolling condition

Bars over symbols denote the average values of the quantities involved for tires A and B.

## APPARATUS

## Test Vehicle

The basic test vehicle consisted of the fuselage and wing center section of a cargo aircraft which was towed tail first by a tractor truck at such an attitude that the original aircraft shock struts were nearly vertical. The original yokes and torque links of the landing-gear struts along with the wheel assemblies were replaced by steel wheel housings which held the tires and wheels tested. These steel wheel housings were connected by an instrumented truss. Holes located in the wheel housing at angular intervals of  $3.5^{\circ}$  permitted the wheel frames to be rotated through a yaw-angle range of  $0^{\circ}$  to  $24.5^{\circ}$  toe out. A sketch of the basic test vehicle is shown in figure 1. A more detailed description of this test vehicle is given in reference 3 and applies in general to the present investigation.

The weight of the test vehicle was adjusted so that the vertical load per tire was approximately equal to 45,000 pounds, and the maximum towing force required was approximately 5,000 pounds per tire.

## Instrumentation

The test vehicle was equipped with instruments for measuring cornering force, self-aligning torque, drag, vertical tire deflection, and horizontal translation. Measurements of these quantities were recorded simultaneously on a 14-channel recording oscillograph mounted in the test vehicle. The oscillograph was equipped with a 0.01-second timer. The instrumentation is discussed in detail in reference 3.

## Tires

General description. - The tires used in this investigation were a pair of  $56 \times 16$  32-ply-rating, type VII, rib-tread tires which were made by the same manufacturer. One tire was new and unused. This tire is referred to in this paper as tire A. The other tire, which will be referred to as tire B, was previously subjected to the static tests which are reported in reference 2. The specifications for these tires, given in table I, were obtained either from reference 7 or by direct measurements made at the end of the tests when the tires were slightly worn.

Tire wear. - Because of the limited number of tests made in this investigation, the tread of the test tires showed little signs of wear at the conclusion of testing. It is felt, therefore, that the effect

on the test results of working and abrading the tires during the course of testing was of a minor nature.

Tire diameter and width. - The variation of the unloaded tire diameter and width with tire inflation pressure is shown in figure 2. It should be noted that the measurements of diameter and width shown in this figure were made after a time lapse of at least 30 minutes following a tire-inflation pressure setting.

#### Test Surface

The yawed-rolling tests were conducted by towing the test vehicle along the center of a 9-inch-thick reinforced-concrete taxi strip. This taxi strip had a slight crown so that the tires on the test vehicle were tilted (less than  $1^{\circ}$ ) with respect to the surface. References 3 and 4 contain profiles of the taxi strip which indicate the surface roughness.

#### TEST PROCEDURE AND EXPERIMENTAL RESULTS

The present investigation of tire characteristics consists of yawed-rolling tests and yawed-rolling relaxation-length tests.

For each run, the test vehicle was moved into towing position on the dry, clean, concrete taxi strip and the wheel housings were rotated and locked at the selected yaw angle. The tires were jacked clear of the ground to remove any residual stresses resulting from the previous runs or from the change of yaw angle on the wheels. After the tires were adjusted to the test inflation pressure, the jacks were removed and the initial vertical tire deflections noted. The vehicle was then towed straight ahead from this initial essentially unstressed condition for a distance of approximately 40 feet. Although the speed remained approximately constant for the duration of each run, it varied from run to run within a speed range of approximately 0.7 to 4.0 miles per hour.

All runs at  $3.5^{\circ}$ ,  $7^{\circ}$ , and  $10.5^{\circ}$  were made with both wheels symmetrically yawed with respect to the longitudinal axis of the test vehicle. The wheels were unsymmetrically yawed for the test runs at  $1.75^{\circ}$ ; that is, one wheel was set at  $0^{\circ}$  and the other at  $3.5^{\circ}$ . During initial towing with the wheels unsymmetrically yawed, the test vehicle first veers off to the side as a result of the unsymmetrical forces. After a short distance, however, the vehicle runs smoothly with its longitudinal axis yawed so that both wheels have the same final intermediate yaw angle of  $1.75^{\circ}$  with respect to the direction of motion.

From the start of each run, continuous recordings were made on measurements of cornering force, self-aligning torque, drag force, vertical tire deflection, and vehicle translation in the direction of motion.

Table II summarizes the test data obtained during the final steady-state stage of the yawed-rolling runs. The variation of normal force  $\bar{F}_{\psi,r,e}$ , self-aligning torque  $\bar{M}_{z,r,e}$ , and pneumatic caster  $q$  with yaw angle is shown in figure 3 for all inflation pressures tested.

The buildup of cornering force with horizontal distance rolled during the initial stages of the yawed-rolling runs for several inflation pressures is illustrated in figure 4. Because of a slight initial residual force or preload in the tires for some of the runs, the original test curves did not always pass exactly through the origin. In consideration of this fact, the test curves shown in figure 4 have been horizontally shifted (where necessary) so that the extrapolation of each curve passes through the origin. These force buildup data were replotted in the manner illustrated in figure 5, and the semilogarithmic plot demonstrates the exponential character of the force buildup. The empirical curve was obtained by fitting a straight line to the data on the semi-logarithmic plot. The corresponding relaxation length for this set of data is, by definition (ref. 3), the rolling distance required for the change in cornering force to decrease by the ratio  $1/e$ . (For example, the relaxation length for the data in figure 5 is 20.3 inches.) The values obtained in this manner from the test runs are listed in table II.

#### PRECISION OF DATA

The instruments used in the tests and the methods of reducing the data are believed to yield results which are, on the average, accurate within the following limits:

Vertical load on tire, $F_z$ , percent . . . . .	$\pm 3$
Cornering force, $F_y$ , percent . . . . .	$\pm 3$
Force perpendicular to wheel plane (normal force), $F_{\psi}$ , percent . . . . .	$\pm 3$
Drag force, $F_x$ , lb . . . . .	$\pm 300$
Self-aligning torque, $M_z$ , lb-in. . . . .	$\pm 3,000$
Tire inflation pressure, $p_0$ or $p$ , lb/sq in . . . . .	$\pm 3$
Outside diameter of free tire, $d$ , in. . . . .	$\pm 0.02$
Horizontal translation in direction of motion, $x$ , percent . . .	$\pm 3$
Vertical tire deflection, $\delta_0$ or $\delta$ , in. . . . .	$\pm 0.2$
Yaw angle, $\psi$ , deg . . . . .	$\pm 0.1$

## DISCUSSION OF PARAMETERS

The variation of steady-state normal force with yaw angle, obtained from the test data is shown in table II and in figure 3. This figure shows that the normal force increased with increasing yaw angle within the test range. With the vertical loading ( $\bar{F}_z \approx 45,000$  pounds) representing approximately 75 percent of the rated vertical load, the normal force did not reach its maximum value within the yaw-angle range tested (up to  $10.5^\circ$ ).

As shown in figure 6, the steady-state cornering force follows substantially the trends that were described for the normal force.

The variation of cornering power with vertical tire deflection and inflation pressure is shown in figure 7. These data, which were derived from the initial slope of the curves for the variation of normal force with yaw angle given in figure 3, indicate that the cornering power decreased with increasing tire deflection and increased with increasing tire inflation pressure for the test range.

The variation of self-alining torque with yaw angle is shown in figure 3 for the vertical loading investigated. The self-alining torque increased with yaw angle until a maximum was reached in the neighborhood of  $7^\circ$ , after which there followed a subsequent decline as yaw angle was further increased within the test range. For constant vertical loading, the data indicate that increasing the inflation pressure tends to reduce the magnitude of the self-alining torque.

The variation of maximum self-alining torque with inflation pressure is shown in figure 8. For the constant vertical loading over the range of inflation pressures investigated, increasing the inflation pressure tends to decrease the maximum self-alining torque.

The variation of pneumatic caster with yaw angle is shown in figure 3. This figure shows that the pneumatic caster is at a maximum at small yaw angles and decreases with increasing yaw angle for the test range covered (up to  $10.5^\circ$  yaw).

The variation of steady-state (rolling condition) drag force with yaw angle is shown in figure 9. These data show that the effect of inflation pressure on drag force for the vertical loading investigated is apparently small. In order to show the trends more clearly, the

ratio of drag force to cornering force  $\frac{\bar{F}_{x,r,e}}{\bar{F}_{y,r,e}}$  is plotted against yaw angle for all test conditions in figure 10. If the resultant horizontal

ground force during yawed rolling were normal to the wheel plane, the drag force  $\bar{F}_{x,r,e}$  would be equal to the cornering force  $\bar{F}_{y,r,e}$  multi-

plied by the tangent of the yaw angle, or  $\frac{\bar{F}_{x,r,e}}{\bar{F}_{y,r,e}} = \tan \psi$ . In figure 10

$\tan \psi$  is represented by the solid line. Since the data do not usually fall along this line, it appears that some force parallel to the wheel plane exists for most of the yaw-angle range investigated.

The variation of relaxation length with inflation pressure is shown in figure 11. Apparently, the relaxation lengths are relatively independent of inflation pressure.

In order to show the effect of ply-rating (measure of carcass stiffness) on yawed rolling tire characteristics, the present test results for a pair of 56-inch, 32-ply-rating tires on cornering power, normal force, self-alining torque, pneumatic caster, and yawed-rolling relaxation length are compared in figure 12 with similar data taken from reference 3 for a pair of 56-inch, 24-ply-rating, type VII tires. This figure shows little difference between the two tires for cornering power, normal force, and yawed-rolling relaxation length and somewhat larger differences for the self-alining torque and pneumatic caster. It appears, in general, that the carcass stiffness or ply-rating effect on the data is of a minor nature.

In further comparison of the present results with previous work, the experimental data of figure 12 show fair agreement with the results that would have been predicted by using the equations developed in reference 6. The solid lines shown in figure 12 are defined by equations obtained from reference 6 and represent the best fit for all type VII tire data available at that time (56 x 16 24-ply-rating, 44 x 13 16-ply-rating, 40 x 12 14-ply-rating, 32 x 8.8 12-ply-rating, and 26 x 6.6 12-ply-rating tires).

#### CONCLUSIONS

Tow tests were made to determine the low-speed yawed-rolling characteristics of two 56 x 16, 32-ply-rating type VII, aircraft tires at a vertical loading approximately equal to 75 percent of the rated vertical loading for these tires. The results of these tests indicated the following conclusions:

1. The normal force increased with increasing angle of yaw within the test range ( $0^\circ$  to  $10.5^\circ$ ).

2. The cornering power decreased with increasing tire deflection and increased with increasing tire inflation pressure for the test range covered.

3. The self-aligning torque increased to a maximum value and then decreased with increasing angle of yaw.

4. The pneumatic caster decreased with increasing angle of yaw for the test range covered.

5. In general, the yawed rolling characteristics followed approximately the same trends reported for other type VII tires and the empirical equations given in NACA Technical Note 4110 were found to predict satisfactorily the magnitudes and variation of these characteristics.

6. Carcass stiffness or ply-rating effects on the yawed-rolling characteristics investigated are generally of a minor nature.

Langley Research Center,  
National Aeronautics and Space Administration,  
Langley Field, Va., October 30, 1958.

## REFERENCES

1. Hadekel, R.: The Mechanical Characteristics of Pneumatic Tyres. S & T Memo. No. 5/50, British Ministry of Supply, TPA 3/TIB, Mar. 1950.
2. Horne, Walter B.: Static Force-Deflection Characteristics of Six Aircraft Tires Under Combined Loading. NACA TN 2926, 1953.
3. Horne, Walter B., Stephenson, Bertrand H., and Smiley, Robert F.: Low-Speed Yawed-Rolling and Some Other Elastic Characteristics of Two 56-Inch-Diameter, 24-Ply-Rating Aircraft Tires. NACA TN 3235, 1954.
4. Horne, Walter B., Smiley, Robert F., and Stephenson, Bertrand H.: Low-Speed Yawed-Rolling Characteristics and Other Elastic Properties of a Pair of 26-Inch-Diameter, 12-Ply-Rating, Type VII Aircraft Tires. NACA TN 3604, 1956.
5. Horne, Walter B., and Smiley, Robert F.: Low-Speed Yawed-Rolling Characteristics and Other Elastic Properties of a Pair of 40-Inch-Diameter, 14-Ply-Rating, Type VII Aircraft Tires. NACA TN 4109, 1958.
6. Smiley, Robert F., and Horne, Walter B.: Mechanical Properties of Pneumatic Tires With Special Reference to Modern Aircraft Tires. NACA TN 4110, 1958.
7. Anon.: Military Specification - Casing; Aircraft Pneumatic Tire. Military Specification, MIL-C-5041, Sept. 16, 1949; Amendment-2, Feb. 8, 1951.

TABLE I.- TIRE SPECIFICATIONS

	Military specification (ref. 7)	End of test, tires in slightly worn condition	
		Tire A	Tire B
<b>Tire:</b>			
Type <sup>a</sup>		VII	
Ply rating		32	
Static load, lb		60,000	
Inflation pressure, lb/sq in.		240	
Burst pressure, lb/sq in.		960	
Moment of static unbalance, oz-in.		90	
Diameter, inflated, in.		54.95 (minimum) 56.40 (maximum)	56.62
Width, inflated, in.		15.40 (minimum) 16.20 (maximum)	56.39
Depth of tread (at tread center line), in.		0.35 (minimum) 0.55 (maximum)	16.15
Casing weight, lb		281	16.26
Tread pattern		Rib	Rib
<b>Inner tube:</b>			
Thickness, in.			0.2
Weight, lb			26.7
<b>Wheel:</b>			
Rim diameter, in.			32.5
Weight, lb			217

<sup>a</sup>Type VII is an extra high-pressure tire.

TABLE III.—YAW TEST DATA

a value not determined.

Value could not be determined.

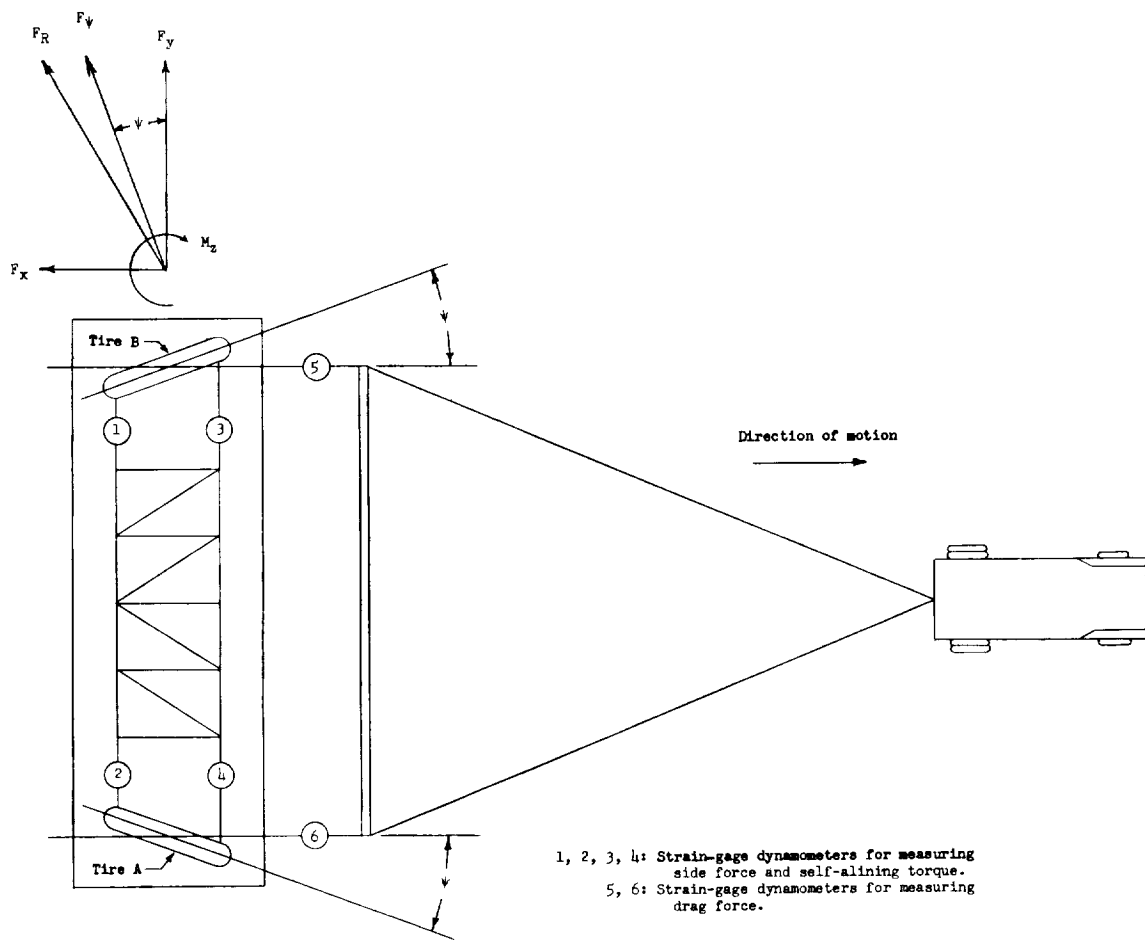


Figure 1.- Sketch of test vehicle.

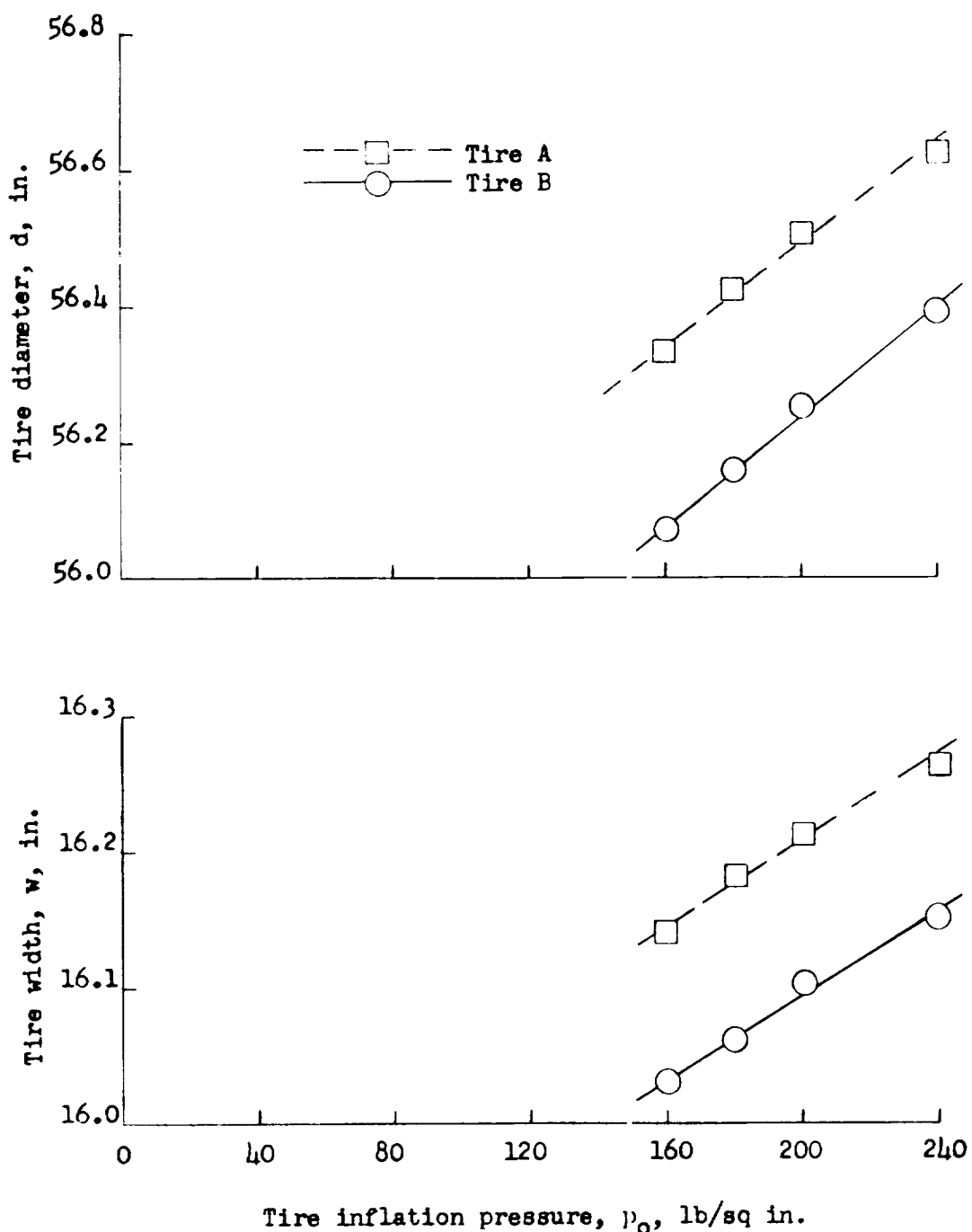


Figure 2.- Variation of free tire diameter and width with tire inflation pressure.

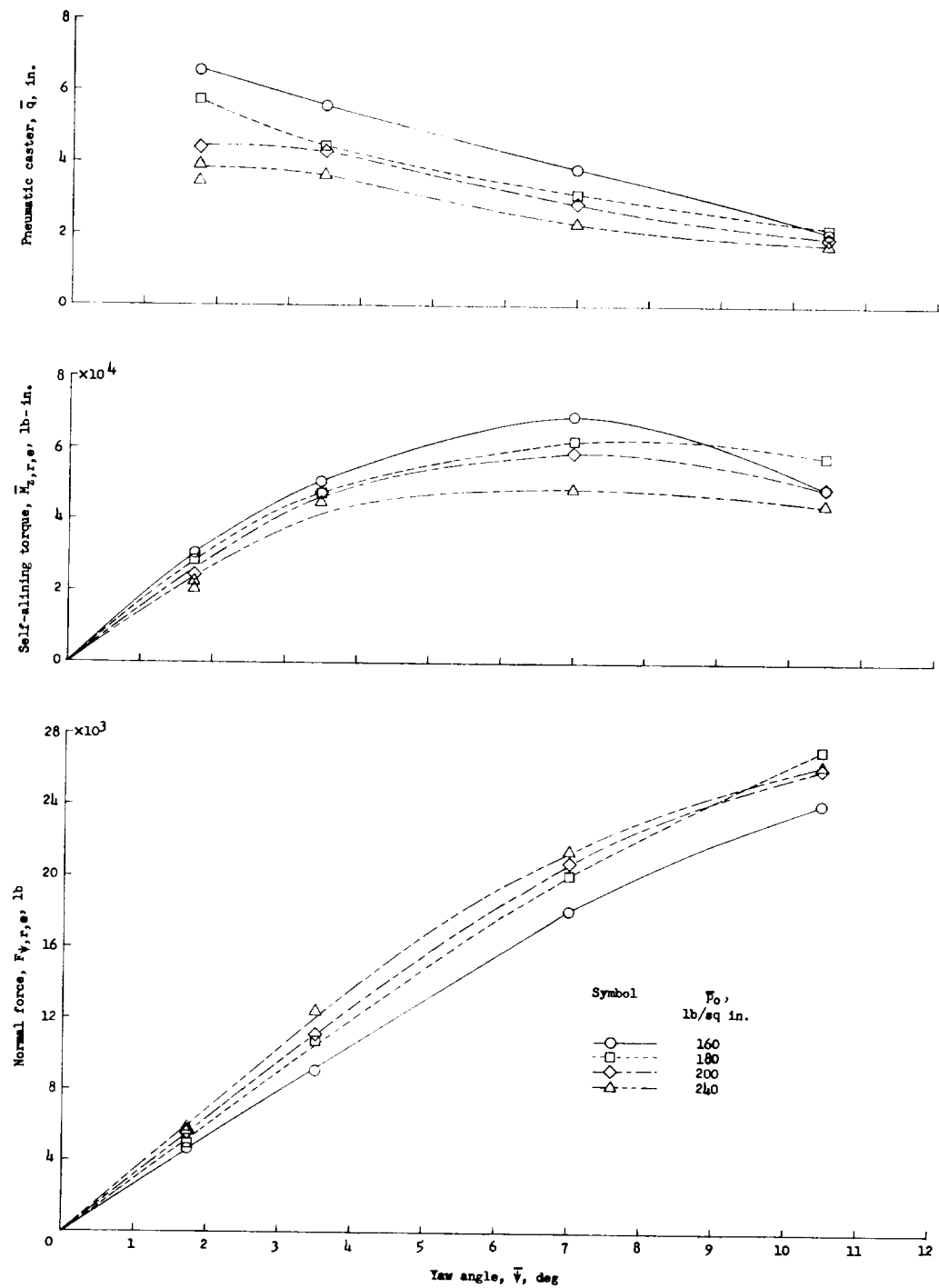
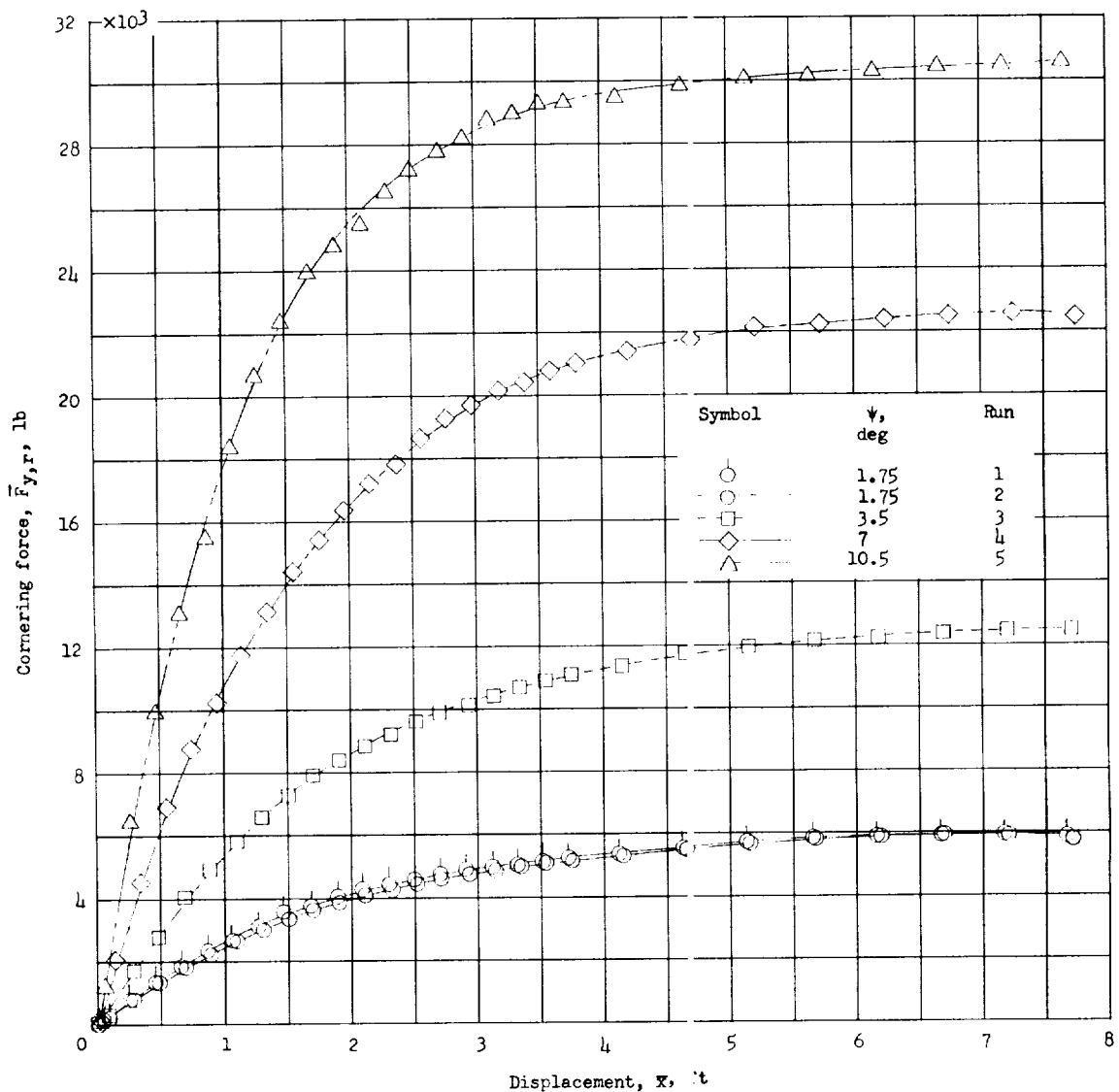
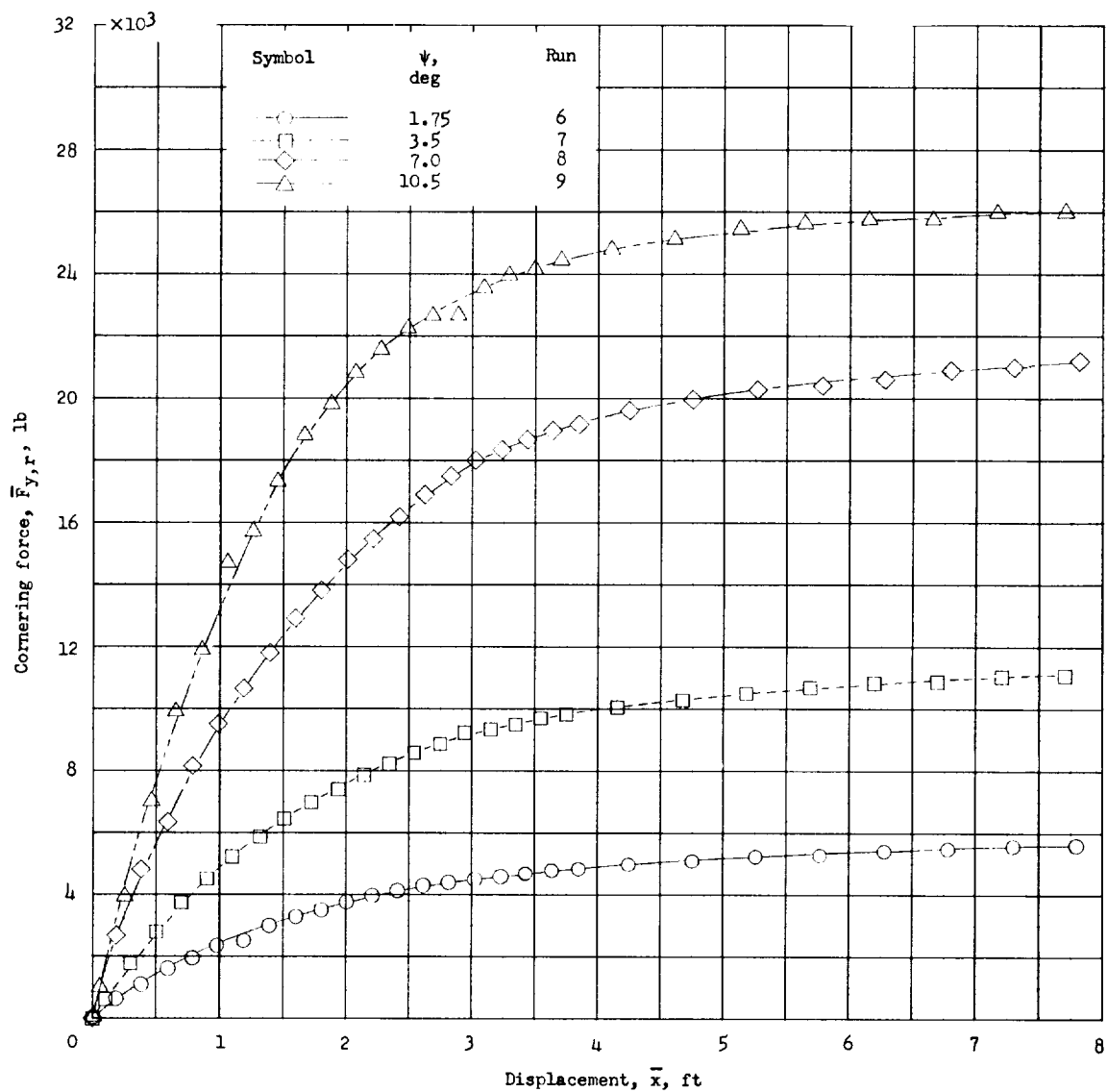


Figure 3.- Variation of normal force, self-aligning torque, and pneumatic caster with yaw angle for the different inflation pressures.



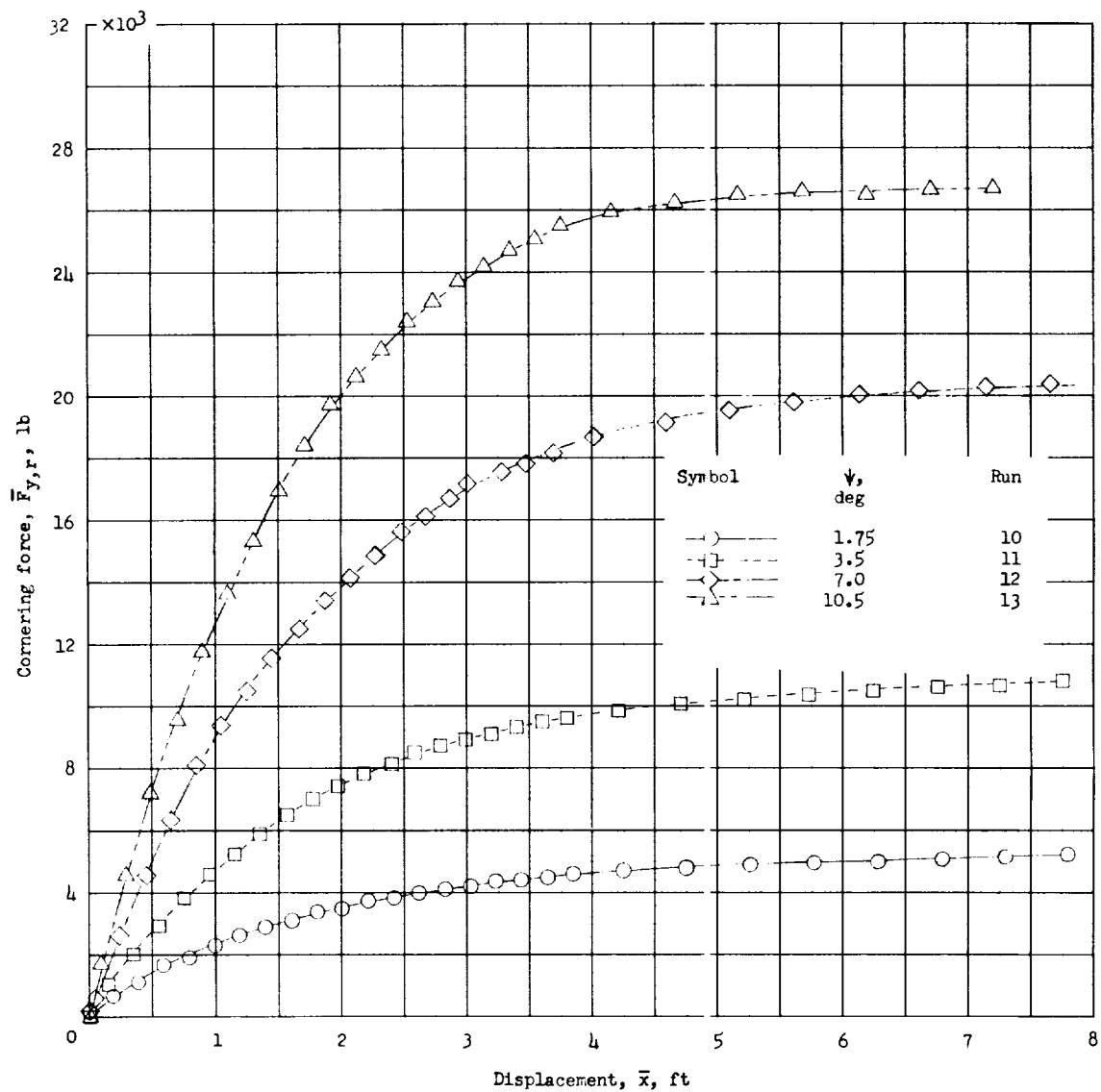
(a)  $\bar{p}_0 = 240$  pounds per square inch;  $\bar{\delta}_0 \approx 3.2$  inches.

Figure 4.- Buildup of cornering force with distance rolled.



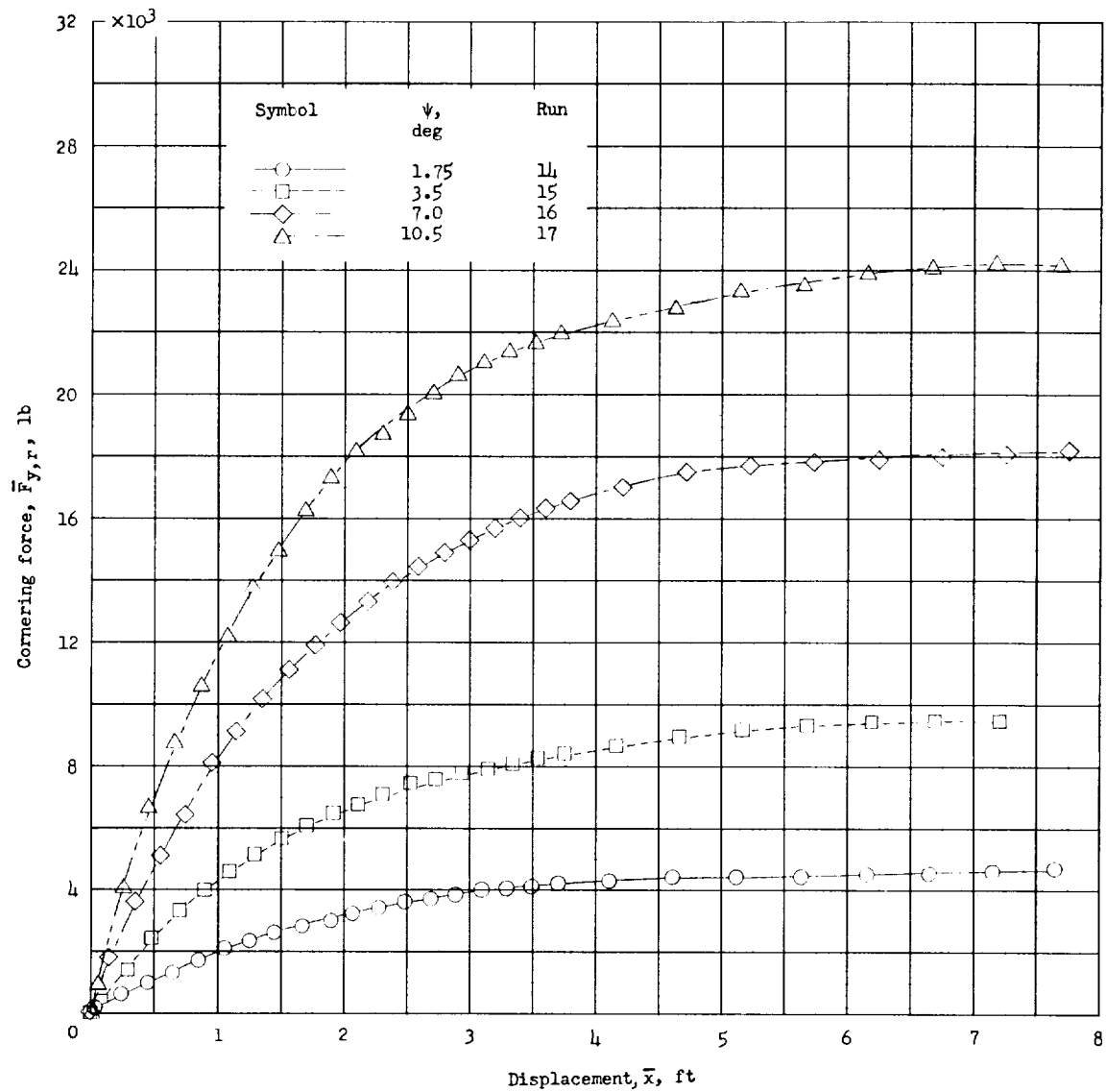
(b)  $\bar{p}_o = 200$  pounds per square inch;  $\bar{\delta}_o \approx 3.5$  inches.

Figure 4.- Continued.



(c)  $\bar{p}_o = 180$  pounds per square inch;  $\bar{\delta}_o \approx 3.7$  inches.

Figure 4.- Continue1.



(d)  $\bar{p}_o = 160$  pounds per square inch;  $\bar{\delta}_o \approx 4.05$  inches.

Figure 4.- Concluded.

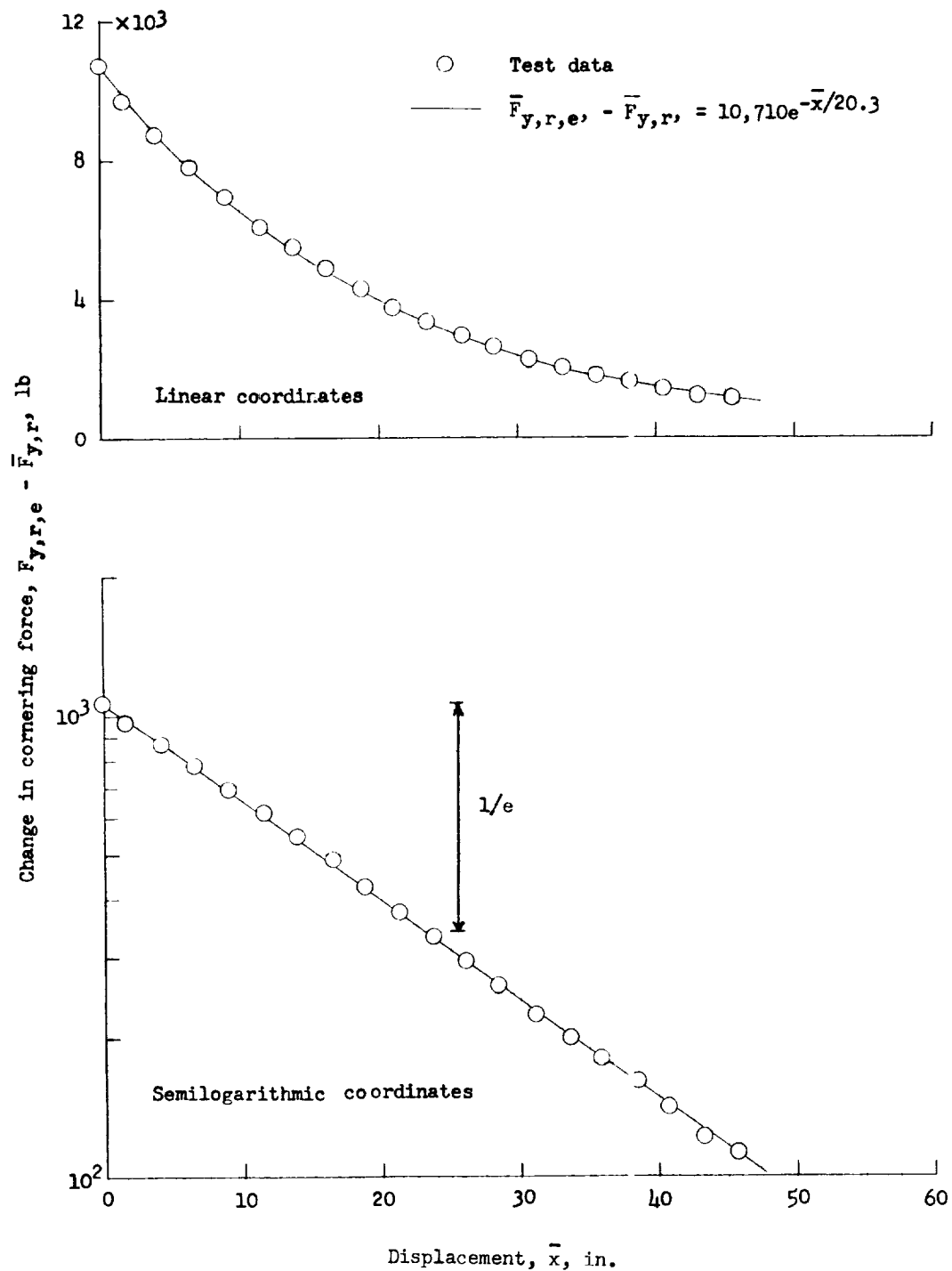


Figure 5.- Experimental data used for determining yawed-rolling relaxation length for run 11.

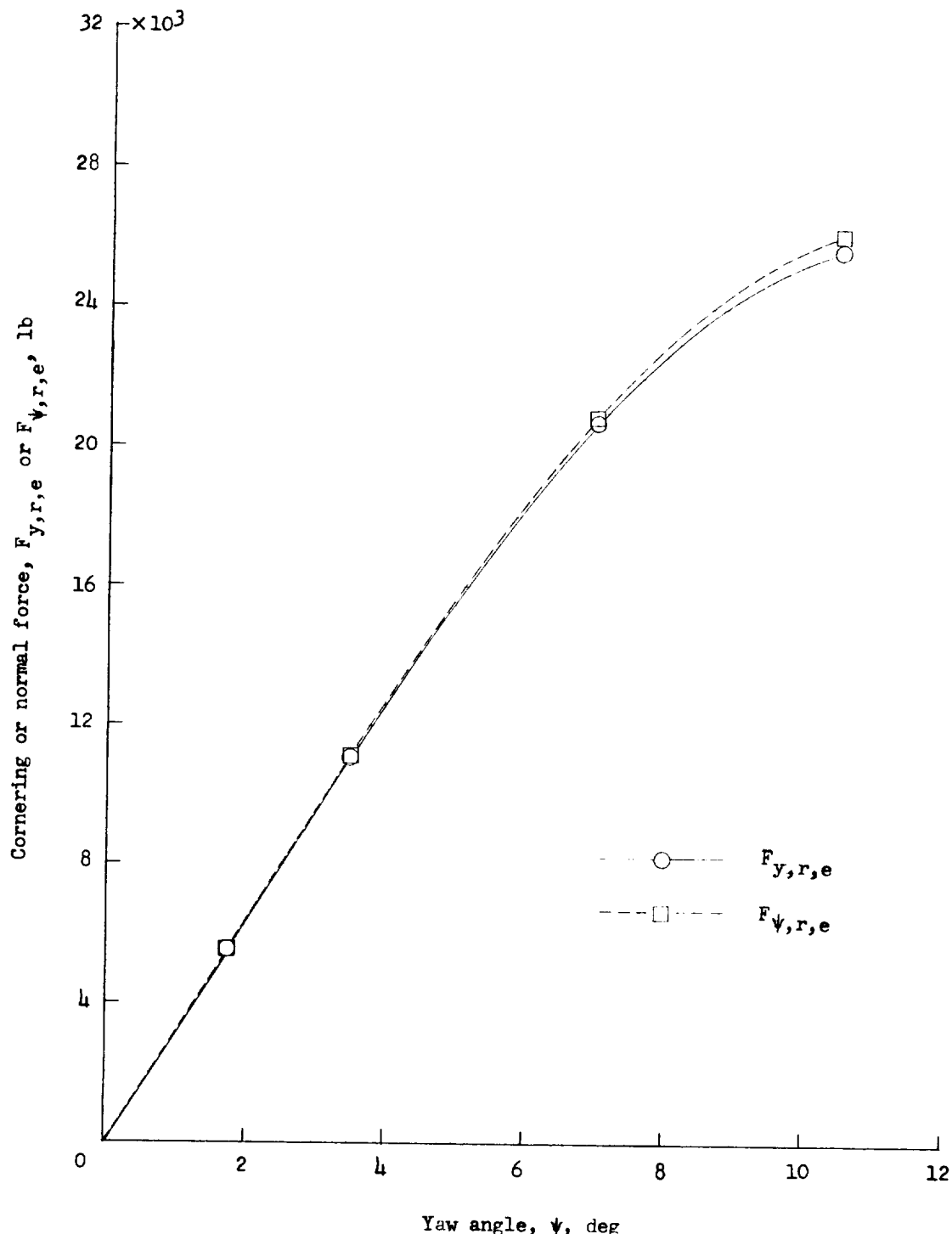
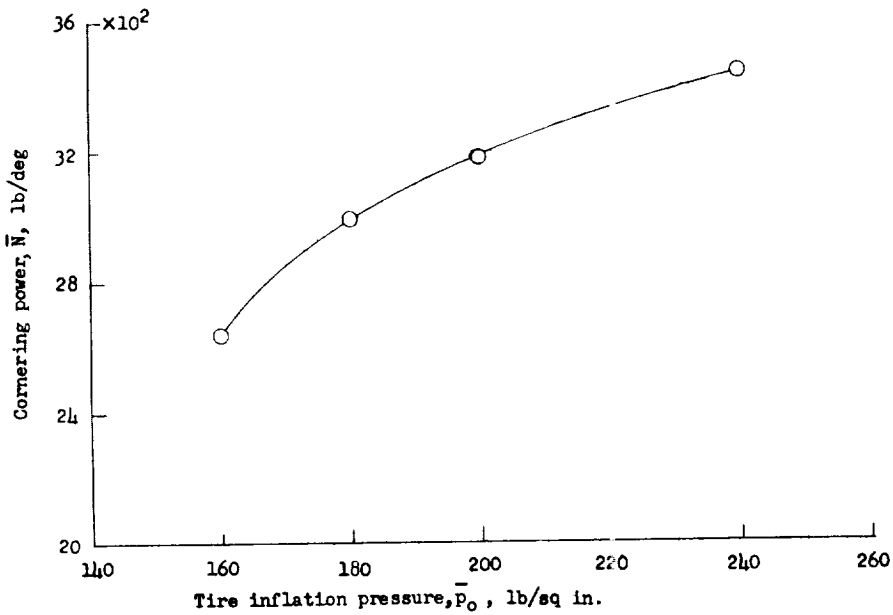
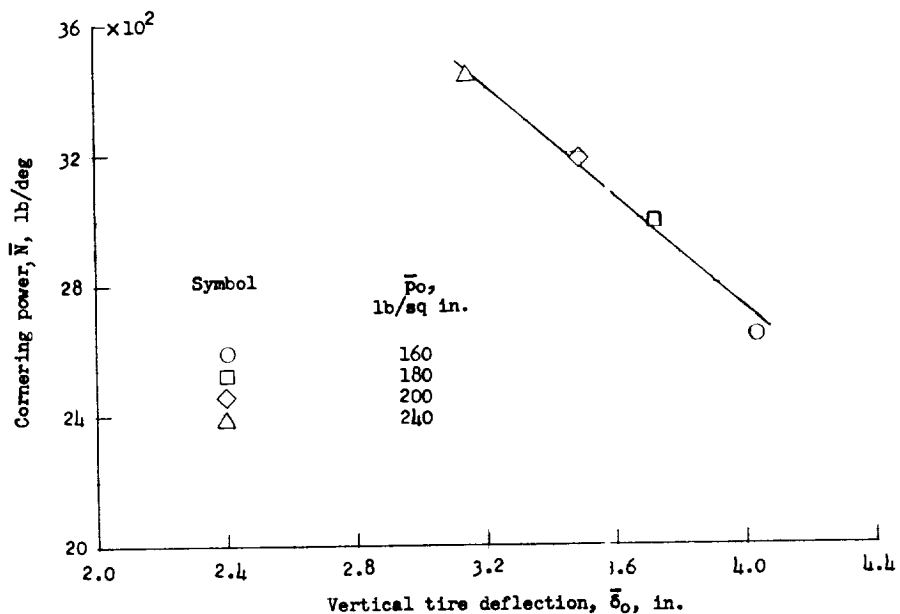


Figure 6.- Comparison of cornering-force and normal-force variations with yaw angle at  $\bar{p}_0 \approx 200$  pounds per square inch.



(a) Variation of cornering power with inflation pressure.



(b) Variation of cornering power with vertical tire deflection.

Figure 7.- Variation of cornering power with vertical tire deflection and inflation pressure.

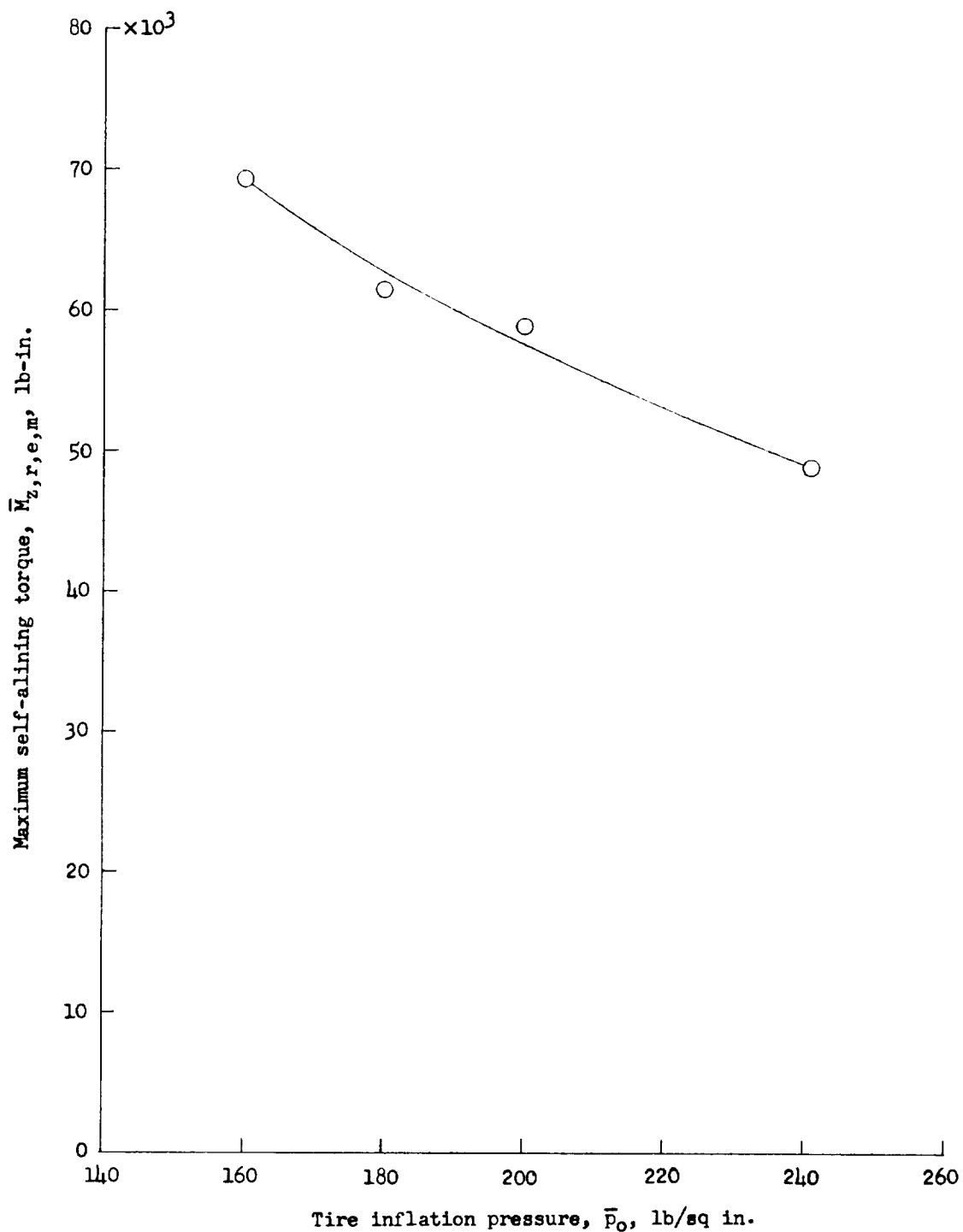


Figure 8.- Variation of maximum self-aligning torque with inflation pressure.

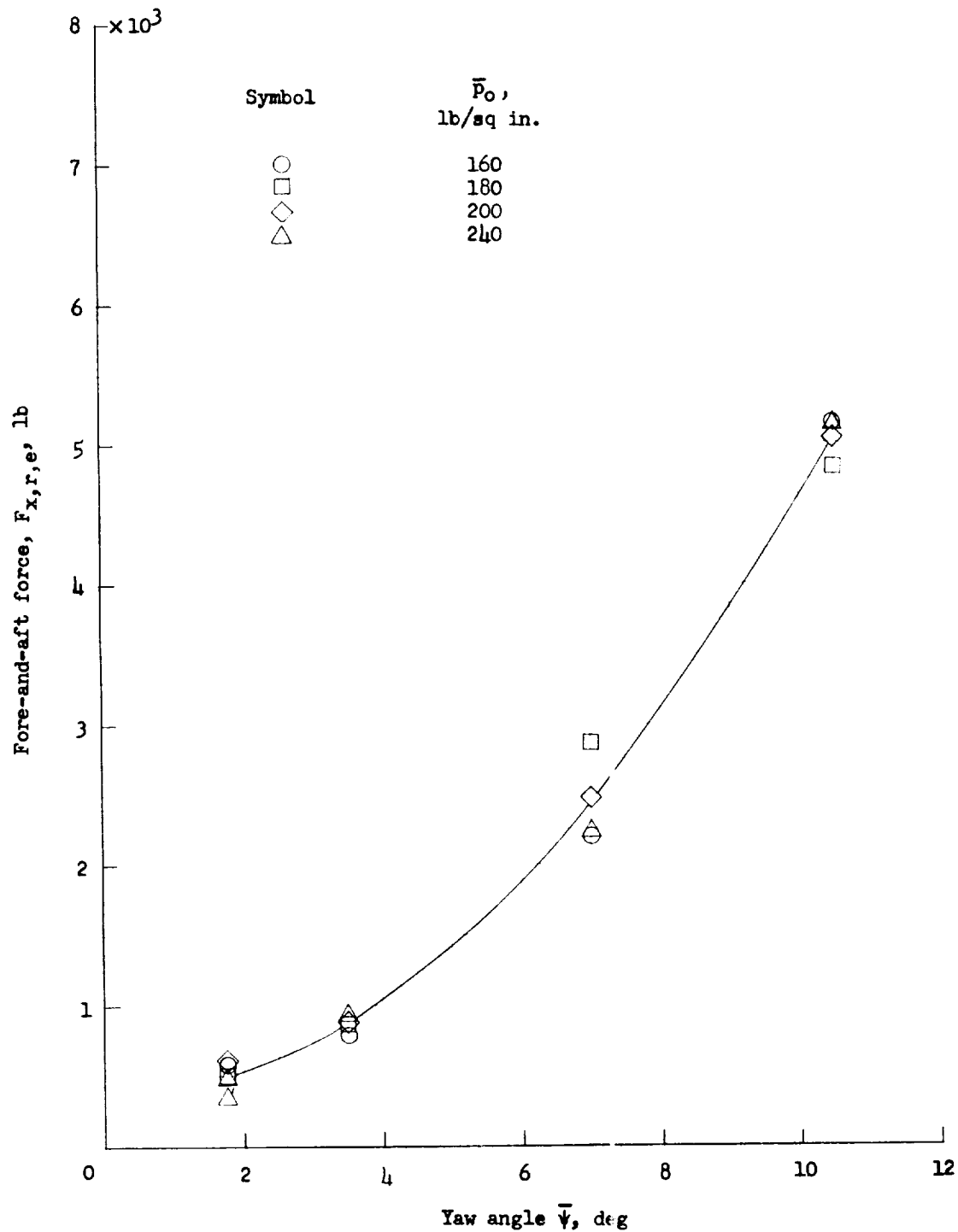


Figure 9.- Variation of drag force with yaw angle for the pressure range tested.

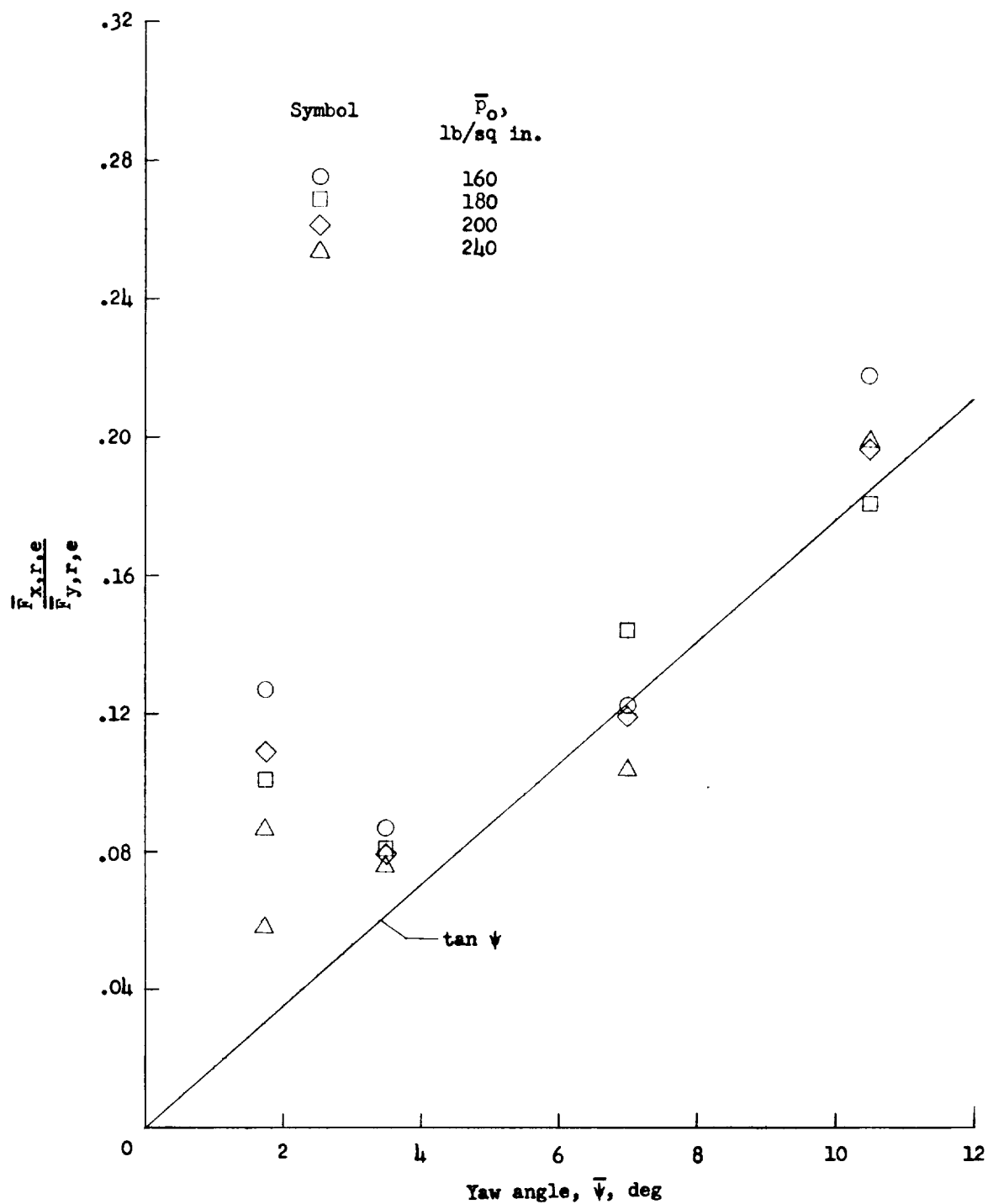


Figure 10. - Variation of the ratio of drag force to cornering force with yaw angle.

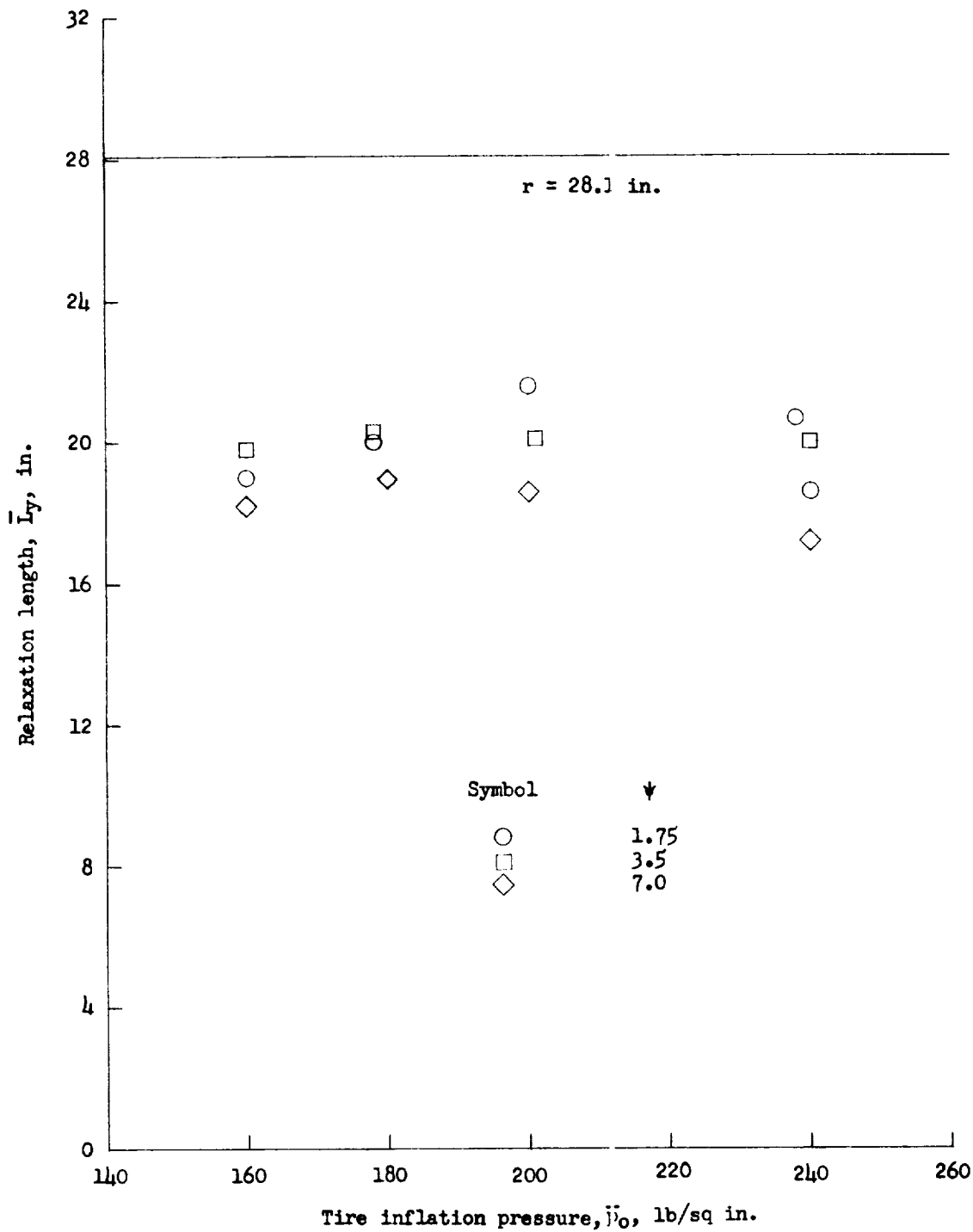
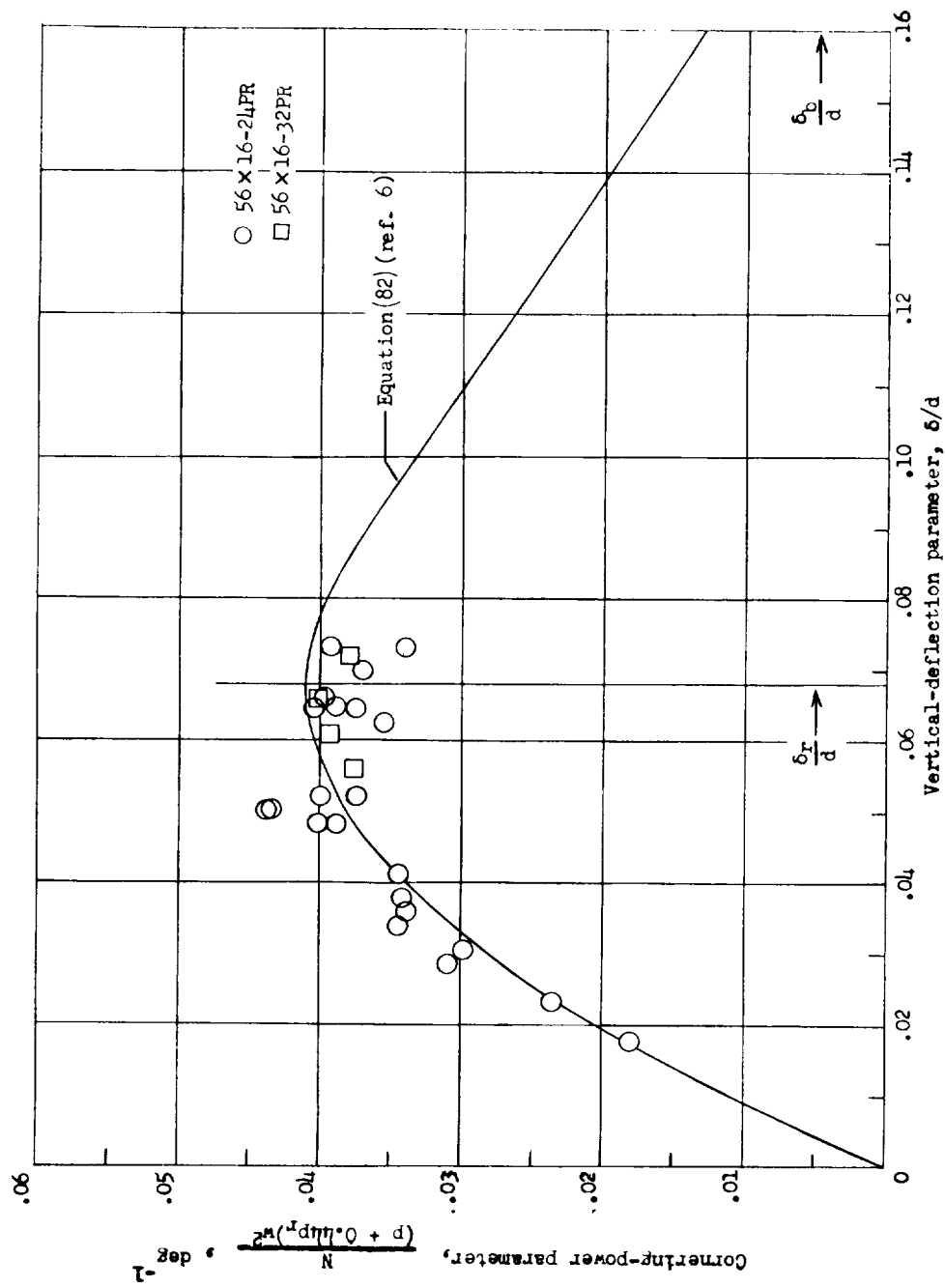
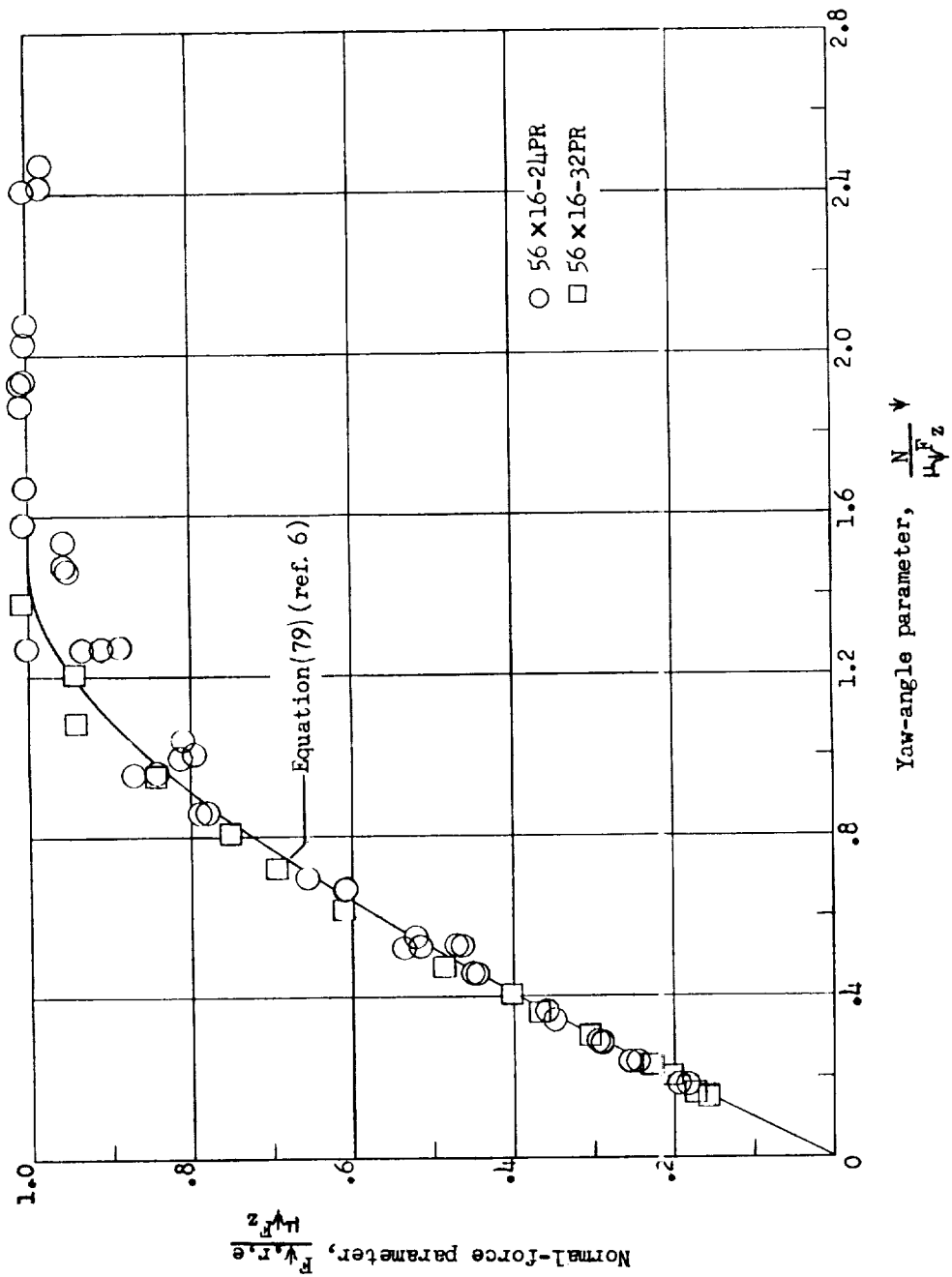


Figure 11.- Variation of relaxation length with tire inflation pressure.



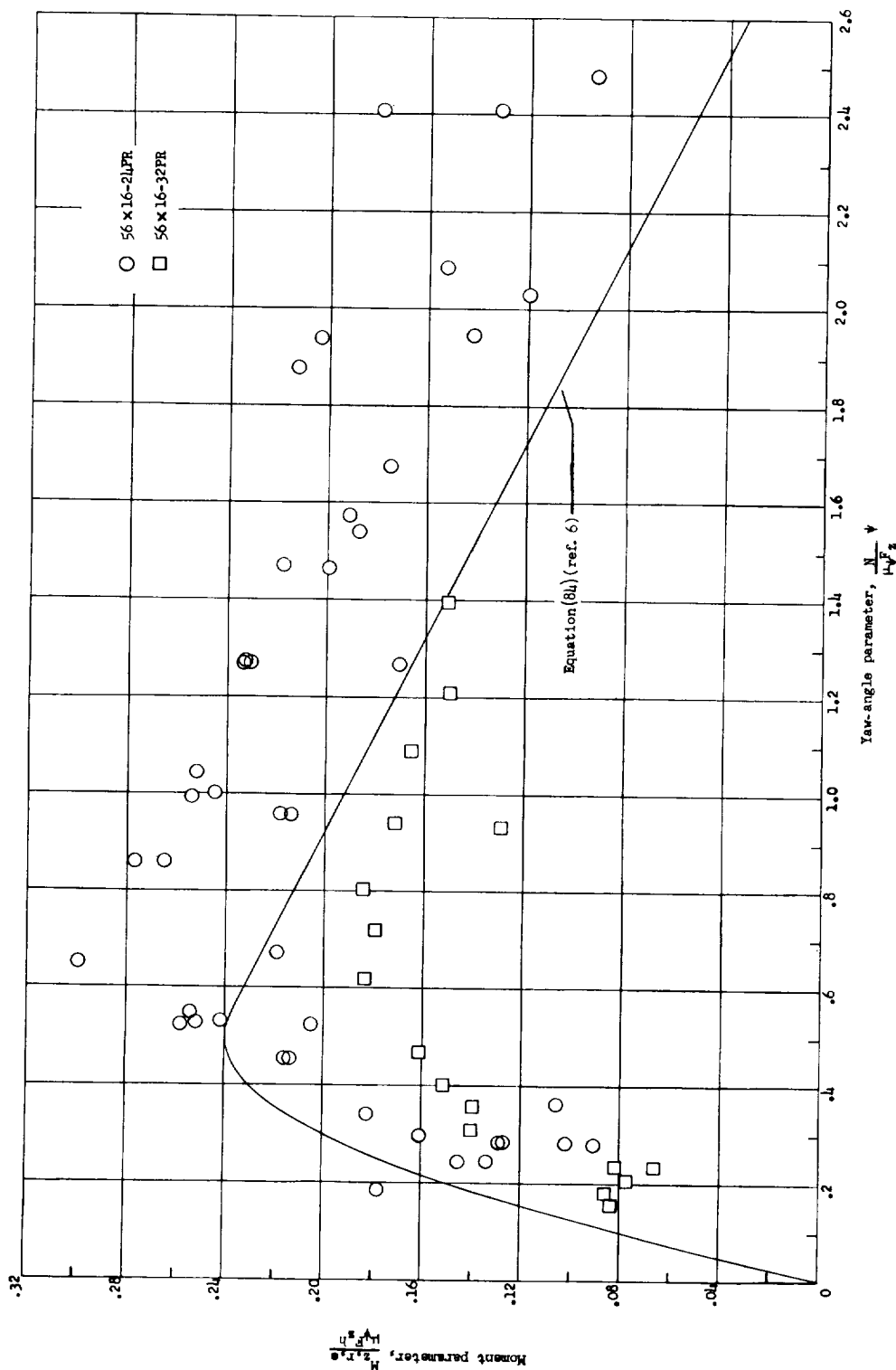
(a) Cornering power.

Figure 12.- Effect of carcass stiffness or ply rating on yawed-rolling characteristics of 32- and 24-ply-rating 56 x 16 type VII aircraft tires.



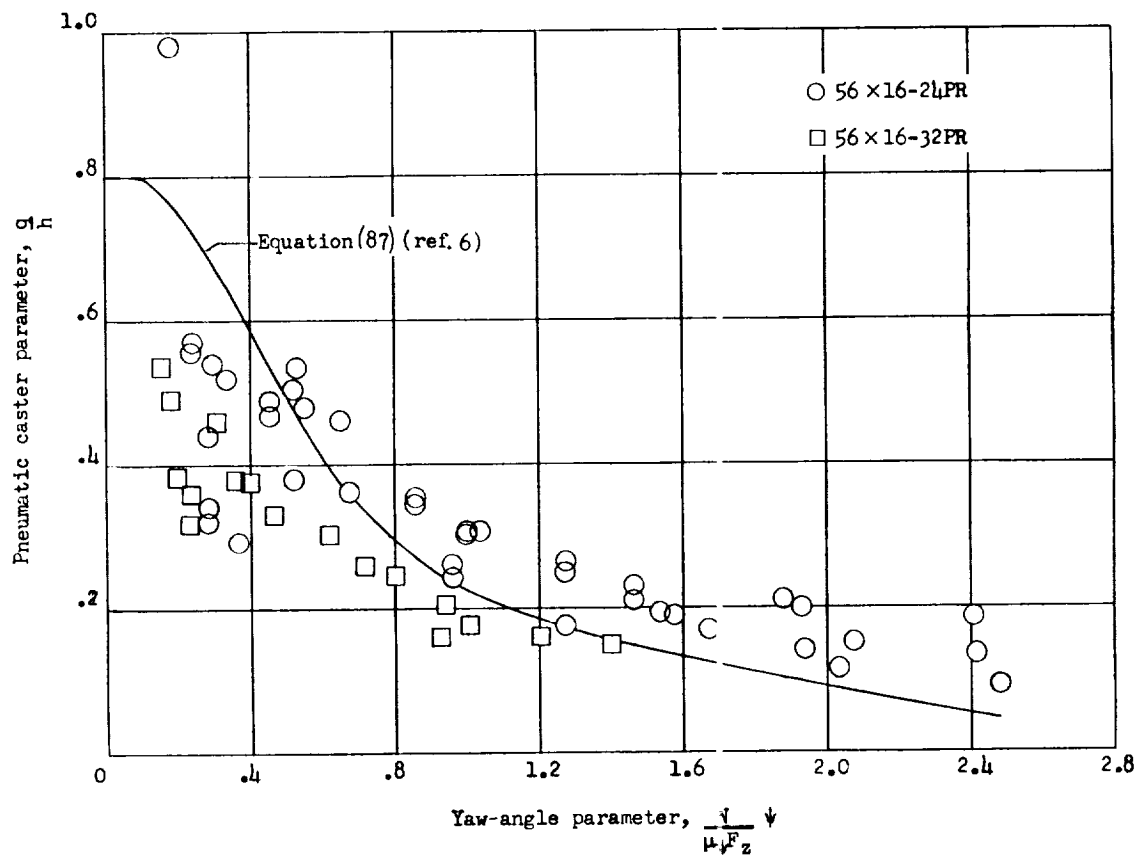
(b) Normal force.

Figure 12.- Continued.



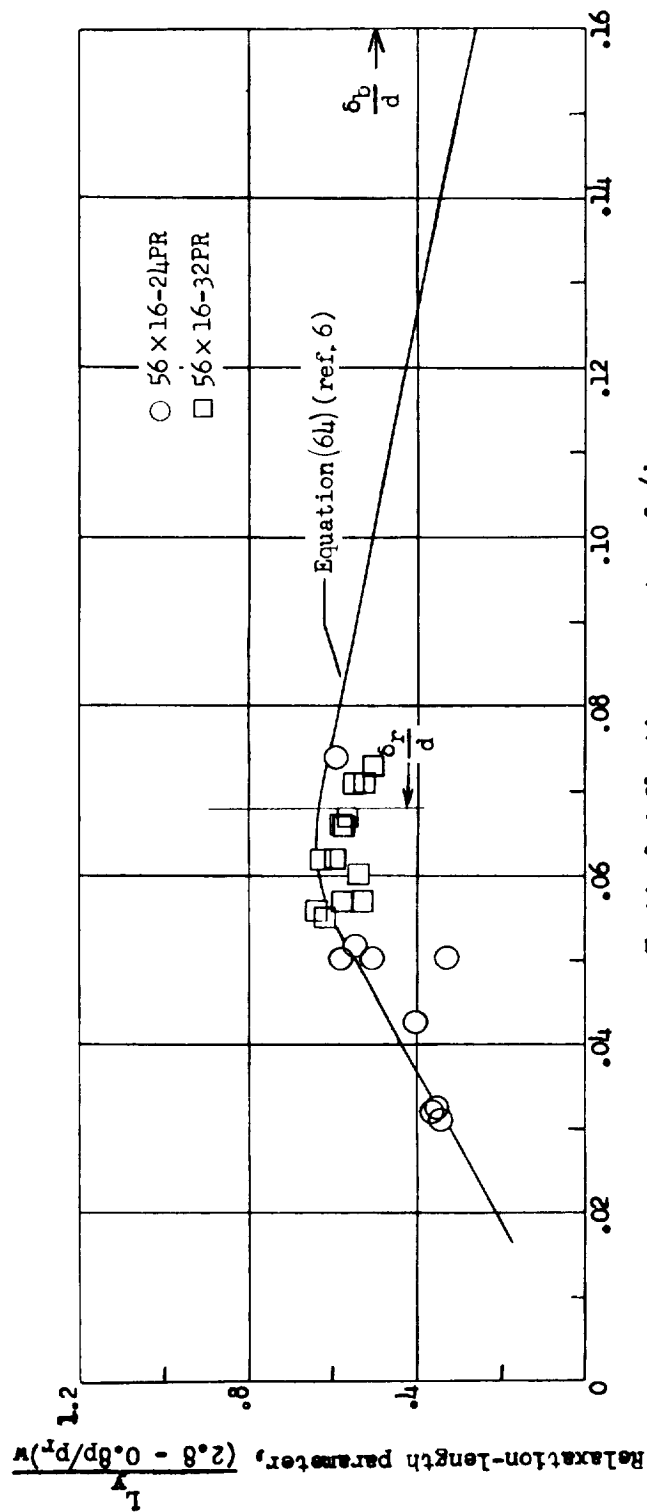
(c) Self-aligning torque.

Figure 12.- Continued.



(d) Pneumatic caster.

Figure 12.- Continued.



(e) Yawed-rolling relaxation length.

Figure 12.- Concluded.

